XPEEM valence state imaging of mineral micro-intergrowths with a spatial resolution of 100nm

A.D. Smith[1], P.F. Schofield[2], A. Scholl[3], R.A.D. Pattrick[4] & J.C. Bridges[2]

[1]CLRC–Daresbury Laboratory, Warrington, Cheshire WA4 4AD United Kingdom
[2]Department of Mineralogy, Natural History Museum, Cromwell Road, London SW7 5BD United Kingdom
[3]Advanced Light Source, Lawrence Berkeley National Laboratory, Berkeley, California CA94720 USA
[4]Department of Earth Sciences, The University of Manchester, Oxford Road, Manchester M13 9PL United Kingdom

A.D. Smith[1], P.F. Schofield[2], A. Scholl[3], R.A.D. Pattrick[4] & J.C. Bridges[2]

Abstract: The crystal chemistry and textural relationships of minerals hold a vast amount of information relating to the formation, history and stability of natural materials. The application of soft X-ray spectroscopy to mineralogical material has revealed that 2p($L_{2,3}$) spectra provide a sensitive fingerprint of the electronic states of 3d metals. In bulk powdered samples much of the textural and microstructural information is lost, but the area-selectivity capability of X-ray Photo-Emission Electron Microscopy (XPEEM) provides the ability to obtain valence state information from mineral intergrowths with a submicron spatial resolution.

Using the state-of-the-art PEEM2 facility on beamline 7.3.1.1 at the Advanced Light Source, Berkeley, USA, a range of minerals, mineral intergrowths and mineralogical textures have been studied for a broad suite of geological, planetary and environmental science materials. High-quality, multi-element valence images have been obtained showing the distribution/variation of the metal valence states across single grains or mineral intergrowths/textures at the 100nm scale and quantitative valence state ratios can be obtained from areas of ~0.01□m^2.

INTRODUCTION

The crystal chemistry and textural relationships of minerals hold a vast amount of information relating to the formation, history and stability of natural materials. Obtaining this from minerals within rocks, meteorites, soils, sediments, mineral-fluid/biota interfaces etc. develops an understanding of both the processes involved in their formation and their reactivity / stability within their current environment. The vast array of mineral assemblages and textural relationships of natural minerals combine with their polygenetic history to render the acquisition of such knowledge a non-trivial exercise.

The 3d transition metals impart a significant influence on mineral properties and behaviour, existing at major, minor and trace concentrations. Knowledge of the multiple valence states exhibited by these metals within mineral assemblages is fundamental to the calculation of geochemical variables such as pressure, temperature and oxygen fugacity. Application of soft X-ray spectroscopy to mineralogical material has revealed that 2p($L_{2,3}$) spectra provide a sensitive fingerprint of the electronic states of 3d metals [1–7].

X-ray Photo-Emission Electron Microscopy (XPEEM) provides sub–micron area-selectivity to obtain valence state information from mineral intergrowths [8]. Using the state-of-the-art PEEM2 facility on beamline 7.3.1.1 at the Advanced Light Source, Berkeley, USA, a range of minerals, mineral intergrowths and mineralogical textures have been studied with spatial resolutions of ~100nm for a broad suite of geological, planetary and environmental science materials.

Chromite in Martian SNC meteorites

Chromite $(Fe^{2+}Mg)(CrAlFe^{3+})_2O_4$ – $(MgFe^{2+})_2TiO_4$ is one of the first minerals to crystallise from basaltic or ultrabasic melts. This, together with its diverse crystal chemistry and Fe^{3+}/Fe^{2+} variation, make it useful for assessing both the degree of melting and oxygen fugacity of the source [9]. Investigations of variations in oxidation of both Fe and Cr across a chromite grain in a Martian SNC meteorite are in progress using XPEEM. This is expected to provide new constraints on oxygen fugacity variation during the earliest stages of crystallization in this Martian system.

Figure 1 shows a XPEEM image of a chromite grain (light) within a pyroxene matrix (dark). Using the area selectivity capability of the XPEEM technique we have extracted Cr $L_{2,3}$ XAS spectra from 6 areas – all ~3x3μm in size – within the grain. XPEEM is a surface sensitive technique, penetrating just a few nm into the surface, and significant surface topography has lead to distortions in photoelectron yield

producing dark regions in the image. The spectra from areas with high photoelectron yield show highly detailed multiplet structure, indicating that the Cr is predominantly in the Cr^{3+} state and located within octahedral sites. The Cr spectra from low yield regions posess a significant noise element, but still demonstrate essentially the same Cr chemistry.

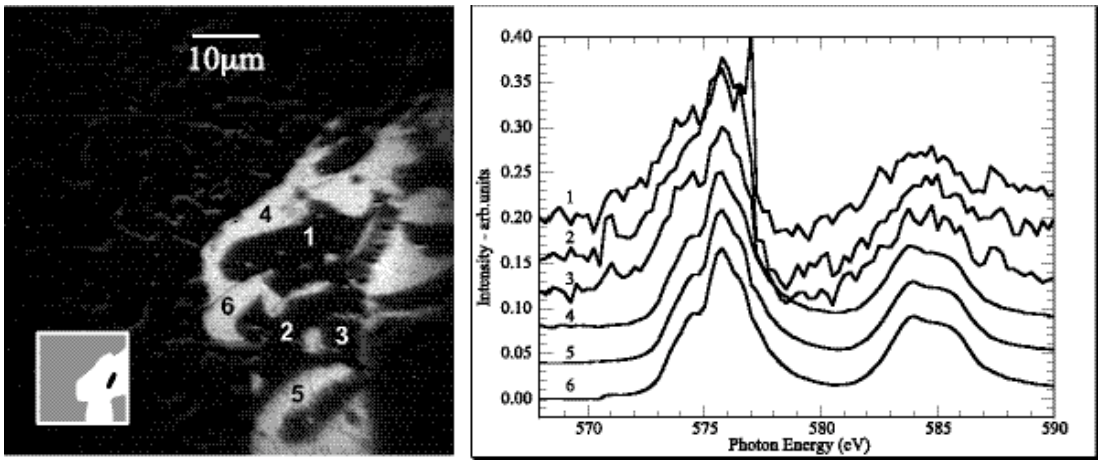

Figure 1 : Cr $L_{2,3}$ spectra from a chromite grain in a martian meteorite. The extent of the chromite grain is indicated in the inset.

Manganese nodules

Manganese nodules from the floor of the deep oceans represent one of the world's great untapped mineral resources [10]. Recent work has focused on the wealth of geochemical information the nodules can provide regarding changes in the ocean chemistry and circulation over the past million years. However surprisingly little is known about the precise nature of the Fe and Mn present in the nodules. The traditional view of the formation of the nodules is also being challenged with the role of microbial activity being seen as crucial in the redox cycles that result in the fixation of Mn and Fe [11,12].

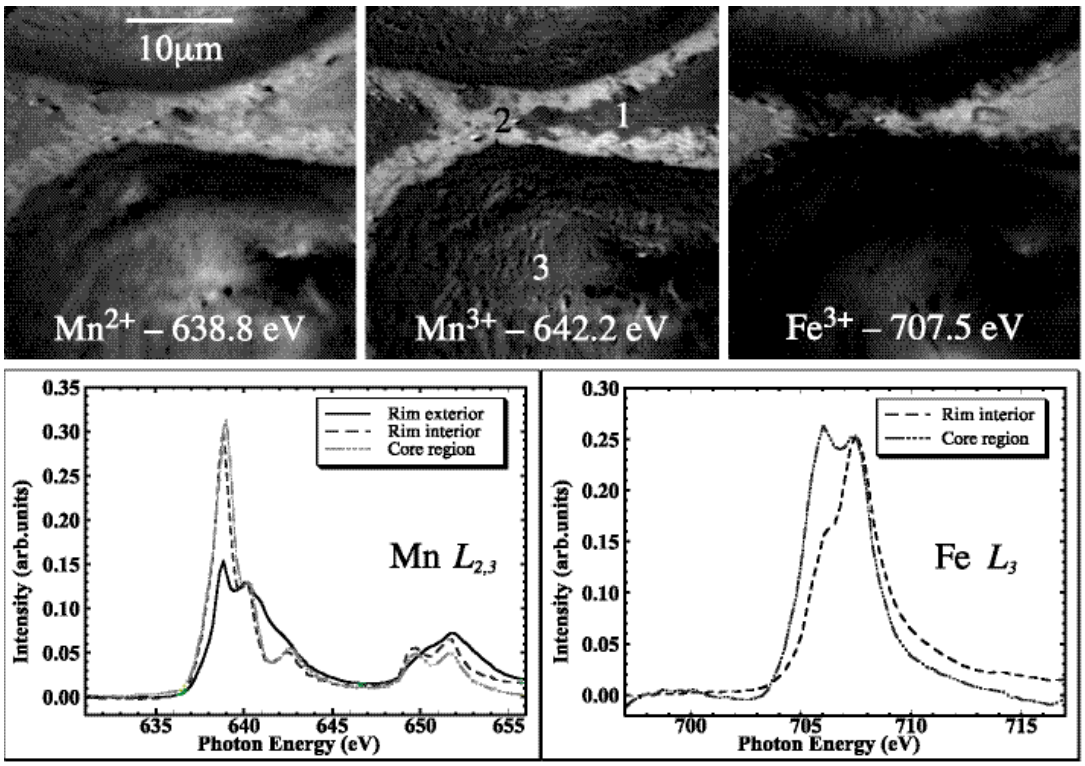

Figure 2 : XPEEM valence images of a growth band within a manganese nodule and corresponding Mn and Fe spectra from different regions, identified in the image as (1) rim interior; (2) rim exterior; (3) 'core' region.

Early XPEEM studies of a nodule from the Madeira Abyssal Plain, Atlantic Ocean – displaying the characteristics of both diagenetic and hydrogenous growth – are shown in Figure 2. The $L_{2,3}$ spectra obtained demonstrate Mn (II, III) and Fe (II, III) oxidation states within a single growth band.

Three regions are seen in the figure; region 1 – rim interior, containing Mn^{2+} with Fe^{3+}, it is possible that this forms zoning between two adjacent growth nodes; region 2 – a Fe free rim exterior comprising a mixture of Mn^{2+} and Mn^{3+}; region 3 - a core region comprising Mn^{2+} with both Fe^{2+} & Fe^{3+}. These differences may be due to differing mineralogy between the 3 regions, or related to redox reactions mediated by sea water interaction or bacterial/microbial activity.

Oxidation of mantle minerals

Volumetrically, approximately 20% of the Earth's lower mantle (~650–2,900km below the surface) comprises magnesiowüstite ((Mg,Fe)O). Although this phase can maintain significant Fe^{3+}, continued oxidation results in the exsolution of magnetite (Fe_3O_4) lamellae along the (100) planes of the magnesiowüstite structure producing a snowflake like or skeletal texture.

The XPEEM image in Figure 3 shows the growth of magnetite (white) in oxidised magnesiowüstite (black). The maximum thickness of the magnetite lamellae is 0.5 μm and excellent imaging of the sub-micron features (100 nm resolution) of the skeletal texture demonstrate the potential of the area selectivity available with this technique.

The image is a chemical state image that has been normalised at 707.6eV, therefore the bright contrast of the lamellae is due to an increased response of the lower energy feature at 706eV compared to the intensity of the higher energy peak.

High quality Fe $L_{2,3}$ XAS spectra have been extracted from areas in the range 0.1 to 5.0 μm^2 across the sample, as indicated in the insets. A third spectrum (dashed) is magnesiowüstite far from the lamellae. The spectra demonstrate a subtle difference between the two minerals with the low energy feature at 706eV being suppressed for the oxidised magnesiowüstite.

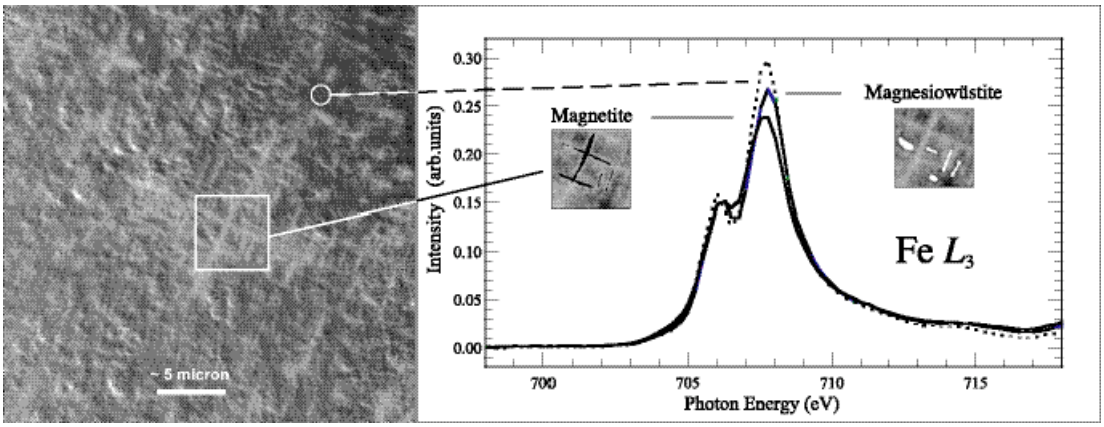

Figure 3 : XPEEM image of magnetite lamellae exsolved in a magnesiowüstite matrix (left) and corresponding Fe $L_{2,3}$ spectra (right). The spectra are obtained from areas less than 200nm wide in and between the lamellae.

Hydrothermal vent sediments

Hydrothermal vents, also known as black smokers, form at mid-ocean ridges of the deep ocean floor and inject superheated, metal bearing sulphidic fluids into cold sea water. As these Fe, Cu and FeCu sulphidic fluids stream out of the vents they mix with cold sea water and preciptiate a complex mineral assemblage of small particles which then settle on the ocean floor. This forms a metal sulphide rich sediment in which the Fe^{2+}/Fe^{3+} & Cu^{2+}/Cu^{+} ratios are likely to be related to the extent of bacterial activity at different horizons around these 'black smoker' deposits. As yet, little is known of the micro–ecology these bacteria live in.

Sediment samples, embedded in epoxy, taken from the vicinity of a hydrothermal vent on the mid-Atlantic ridge have been studied. Figure 4 shows XPEEM images of the Fe and Cu distributions within the sample. Along with Fe sulphides, several Cu–Fe growth nodules with alternating Fe and Cu rich zones also feature. The Fe $L_{2,3}$ spectra represent 3 iron bearing phases : a low textured Fe sulphide (centre right) with a single peak at 705.5eV (spectra 1,2); a broken iron oxide structure (lower right) with a distinct second feature at 707.2eV (3,4,5); and the Cu zoned region with a shoulder at 707.2eV (6,7).

The Fe spectra (1,2) are from an Fe sulphide mineral, the broken region (3,4,5) is oxidised, possibly due to microchemical interaction with the sea water at grain boundaries and nodules of Fe intergrown with Cu (6,7) is mostly in the form of a Cu–Fe sulphide.

Copper spectra from these growth zones all display a structure characteristic of Cu(I). This indicates a lack of oxidation in the growth of these chemically banded nodules at high temperatures close to the vent.

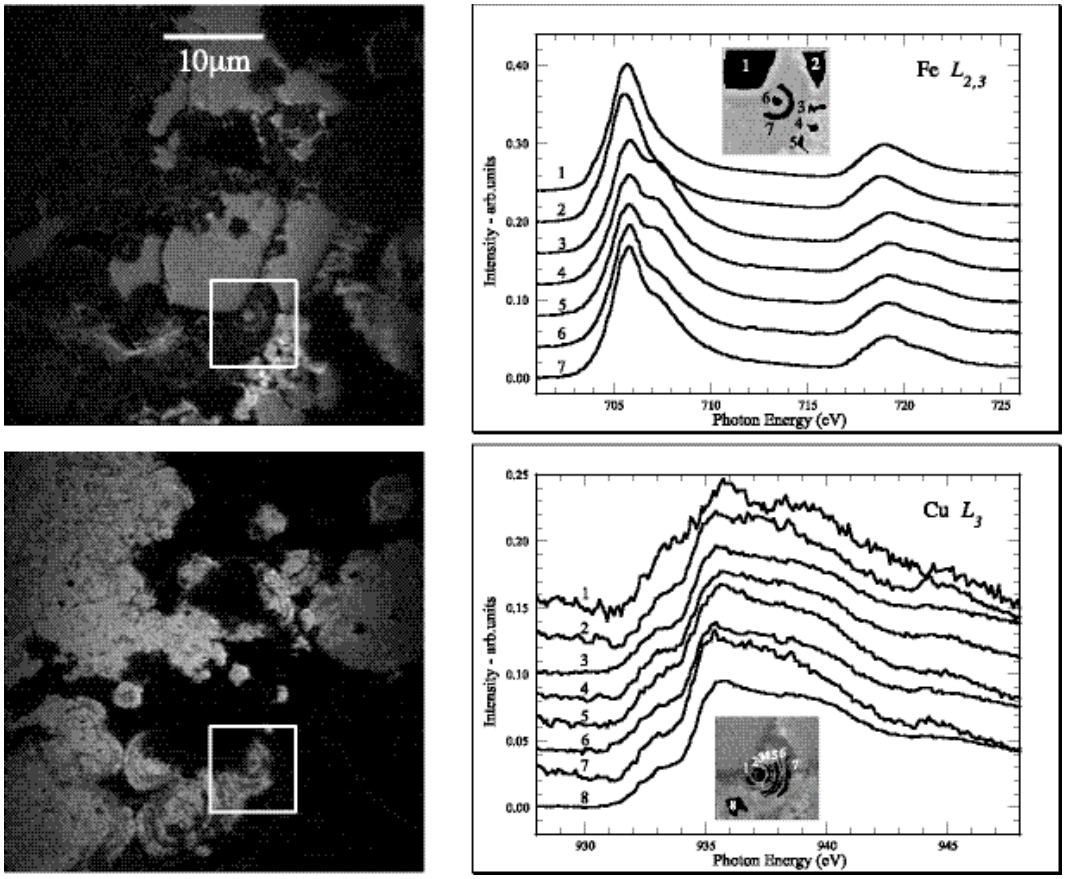

Figure 4 : XPEEM images of Fe (top) and Cu (bottom) distributions in a sediment sample collected from the neighbourhood of a mid-Atlantic hydrothermal vent. Fe $L_{2,3}$ & Cu L_3 spectra from regions within the 10□m x 10□m box shown reveal differences in iron oxidation states, but the copper phases of band within the grain shown are the same.

Acknowledgements

ADS and PFS acknowledge funding from NERC and Daresbury Laboratory via the EnviroSynch project for travel and subsistance.

The Advanced Light Source is supported by the Director, Office of Science, Office of Basic Energy Sciences, Materials Sciences Division, of the U.S. Department of Energy under Contract No. DE-AC03-76SF00098 at Lawrence Berkeley National Laboratory.

References

[1] Cressey G., Henderson C.M.B., and van der Laan G. *Phys.Chem.Minerals* **20** (1993) 111
[2] Henderson C.M.B., Redfern S.A.T., and Cressey G. *Rad.Phys.Chem* **45** (1995) 459
[3] Schofield P.F., Henderson C.M.B., Cressey G. and van der Laan G. *J.Synchro.Rad.* **2** (1995) 93
[4] van der Laan G., and Kirkman I.W. *J.Phys.:Conden.Mat* **4** (1992) 4189
[5] Schofield P.F., van der Laan G., Henderson C.M.B., and Cressey G. *Mineral.Mag.* **62** (1998) 65
[6] Pattrick R.A.D., van der Lann G., Henderson C.M.B., and Vaughan D.J. *J.Phys.Chem.Min.* **20** (1993) 395
[7] van der Laan G., Pattrick R.A.D., Henderson C.M.B., and Vaughan D.J. *J.Phys.Chem.Solids* **53** (1993) 1185
[8] Smith A.D., Cressey G., Schofield P.F. and Cressey B. *J.Synchro.Rad* **5** (1998) 1108
[9] Herd C. D. K. et al. *Am. Mineral.*, **86** (2001) 1015-1024.
[10] Takematsu N., Sato Y and Okabe S. *Marine Chem.* **26** (1989) 41-56.
[11] Ninfopoulos M.K., and Pattrick R.A.D., *Mineral.Mag.* **55** (1992) 423